Semiconductor Science and Technology

PAPER

Thermal boundary resistance of direct van der Waals bonded GaN-on-diamond

OPEN ACCESS
IOP Publishing
Semiconductor Science and Technology
Semicond. Sci. Technol. **35** (2020) 095021 (6pp)
https://doi.org/10.1088/1361-6641/ab9d35

Thermal boundary resistance of direct van der Waals bonded GaN-on-diamond

William M Waller[1], James W Pomeroy[1,3], Daniel Field[1], Edmund J W Smith[2], Paul W May[2] and Martin Kuball[1]

[1] Center for Device Thermography and Reliability, HH Wills Physics Laboratory, University of Bristol, Bristol BS8 1TL, United Kingdom
[2] School of Chemistry, University of Bristol, Bristol BS8 1TS, United Kingdom

E-mail: james.pomeroy@bristol.ac.uk

Received 27 March 2020, revised 11 June 2020
Accepted for publication 16 June 2020
Published 4 August 2020

Abstract

Carbide forming interlayers, such as amorphous silicon nitride, are typically used for GaN-on-diamond heterogenous integration. This interlayer has a low thermal conductivity, introducing an additional extrinsic interfacial thermal resistance. It may therefore be advantageous to omit this layer, directly bonding GaN-to-diamond (van der Waals bond). However, weakly bonded interfaces are known to increase the intrinsic thermal boundary resistance. An adapted acoustic mismatch model has been implemented to assess which bonding approach is the most optimal for low thermal resistance GaN-on-diamond. A high thermal boundary resistance of 200 m^2 K GW^{-1} is predicted for weakly bonded GaN-to-diamond interfaces, which is close to the measured value of 220 $\pm$ 70 m^2 K GW^{-1}, and $\sim$7$\times$ higher than values measured when a 10's nm-thick SiN interlayer is included. Covalently bonded interfaces are therefore critical for achieving low thermal resistance GaN-on-diamond.

Keywords: GaN-on-diamond, 2D materials, thermal barrier, phonon transmission, van der Waals, wafer bonding, acoustic mismatch model

(Some figures may appear in colour only in the online journal)

1. Introduction

Electrically active device layers are often attached to higher thermal conductivity materials for improved thermal management. The intrinsic interfacial thermal boundary resistance (TBR), also known as Kaptiza resistance, is determined by the rate of phonon propagation across an interface. Consequently, TBR must be considered carefully when designing an electronic device. This is particularly important for 2D materials such as graphene [1] and boron nitride (BN) [2] which have very dissimilar phonon density of states to those of bulk materials. To improve thermal dissipation from active devices, semiconductor layers are often attached to diamond wafers [3] or to other higher thermal conductivity materials, such as GaAs and SiC [4], which act as heat spreaders/sinks. Diamond is an ideal heat spreading material, having the highest bulk thermal conductivity (2200 W m^{-1} K^{-1}). Recent examples of heterogeneous integration with diamond heat spreaders are GaN-on-diamond [3, 5, 6] and Ga_2O_3-on-diamond [7]. GaN-on-diamond uses high thermal conductivity polycrystalline diamond ($\sim$1200-1500 W m^{-1} K^{-1}) instead of the SiC ($\sim$440 W m^{-1} K^{-1}) substrates conventionally used for high-power RF GaN transistor heteroepitaxy [5, 6]; this enables 3$\times$ increase in RF transistor areal output power density with respect to conventional GaN-on-SiC [8]. Thermal boundary resistance is especially a concern for GaN-on-diamond transistors operating at ultra-high-power densities. Gallium does not readily form a carbide bond, so there are two options for bonding GaN and diamond: (1) Including a carbide forming bonding interlayer which improves adhesion [9], *e.g.* low thermal conductivity silicon nitride (1–2 W m^{-1} K^{-1}), but

[3] Author to whom any correspondence should be addressed.

introduces an additional thermal resistance; (2) Direct van der Waals (vdW) bonding without an interlayer. It is currently unclear whether option 1 or 2 is the optimum solution for GaN-on-diamond, *i.e.* which has the lowest total thermal resistance. To make this assessment we have implement a weakly bonded TBR model for GaN-on-diamond and use transient thermoreflectance (TTR) for experimental confirmation.

GaN-on-diamond is usually fabricated by removing the original growth substrate, depositing the aforementioned interlayer, such as SiN, on the back side of the GaN, and then growing polycrystalline diamond [3]. The total effective thermal boundary resistance (TBR_{eff}) is a lumped term, including the intrinsic TBR at each interface, the resistance of the thin-film SiN layer, and the resistance due to the diamond nucleation layer which is usually composed of a few 10 s of nm of poor-quality, small-grained diamond [10]. Despite it being typically only a few 10 s of nm thick, the SiN contributes most of the GaN-on-diamond interface thermal resistance, resulting in a TBR_{eff} >30 m^2 K GW^{-1}, which adds >20% to the total device resistance [6]. While direct diamond on GaN growth has been demonstrated [11], there are no reported TBR assessments for this case, although it generally known that more weakly bonded interfaces result in a higher TBR [12]. Indeed, a high TBR value of ∼60 m^2 K GW^{-1} has been measured for Ga_2O_3 vdW bonded to diamond [7]. This is 2× higher than the TBR_{eff} value measured for GaN-on-diamond including a SiN interlayer.

There are several different modelling approaches for predicting the TBR of weakly bonded interfaces. *Ab initio* density functional theory (DFT) [13] or molecular dynamics (MD) [12] can give insights at the atomic level, although these methods are computationally complex and require experimental calibration. Analytical models, based on the phonon mismatch between dissimilar materials, are more commonly used for TBR assessment. The diffuse mismatch model (DMM), which is usually a good approximation of the TBR for solid-solid interfaces at room-temperature, is based on the overlap between the phonon density of states for the two materials in contact and assumes a 'welded' (fully covalent) interface. The DMM prediction for a GaN-to-diamond interface is negligible, <5 m^2 K GW^{-1} [6], which suggests that direct GaN-to-diamond bonding, without an intermediate layer, may be the lowest thermal resistance solution. Similarly, the TBR value of Ga_2O_3-on-diamond predicted by DMM is 3 m^2 K GW^{-1}, whereas the measured TBR is 20× higher [7]. In both DMM estimations the interfacial bonding strength has not been accounted for when calculating TBR, and consequently DMM severely underpredicts the TBR. Alternatively, the acoustic mismatch model (AMM), assumes specular phonon reflection, with the only parameters being the bulk acoustic properties of the materials [14]. Models of acoustic transmission at linear slip interfaces have been developed and are used routinely in seismology [15]. Prasher *et al* applied a simplified form of these equations to predict the TBR of weakly bonded Si/Si and Si/Pt interfaces [16], but without experimental verification of the model. More recently, Prasher *et al* extended this approach to consider a weakly bonded interface under high pressure [17]. There have been other models which consider the thermal barrier under pressure, notably by Gotsmann *et al*, who developed a model of quantized thermal transport at rough interfaces [18].

In this work we implement a full AMM treatment of a weakly bonded interface and use this to predict the TBR of a direct GaN-to-diamond interface. This model requires only the phonon properties of each material and the strength of van der Waals bond between the materials (adhesion energy) to be known. The adhesion energy parameter can be determined by shear 'peel off' type tests [19], for example. This will enable us to answer the question of whether 'adhesion layers' or 'seeding layers' such as SiN are beneficial and/or necessary for efficient heat transport. The theoretical model developed here is applied to GaN-on-diamond, although it is generic and can be used to analyze other weakly bonded materials.

2. Experimental details

TBR was measured for 2 μm polycrystalline diamond films deposited onto three standard GaN-on-Si wafers, with a GaN layer thickness of 1.03 μm deposited by MOCVD. The Ga-polar GaN surfaces were pre-seeded with a mixture of micro- and nano-diamond using an electrostatic spray technique and the diamond then grown by microwave plasma-enhanced chemical vapour deposition (MWCVD) in a 1.5 kW, 2.45 GHz ASTeX-type reactor. CVD was performed in a methane/hydrogen plasma (4% CH_4 in H_2) with MW input power of 1100 W, chamber pressure of 110 Torr for 4 h. More details about the reactor design and growth method are given in Ref. [20]. Low growth temperatures (∼750 °C) were used to reduce the internal strain in the diamond film after growth resulting from the thermal expansion mismatch between diamond and GaN, thereby reducing the risk of cracking or delamination.

In order to perform TTR measurements, a 100 nm thick Au transducer layer was deposited onto the diamond, together with a 10 nm thick Cr adhesion layer, using the equipment and method described in [6] and [21]. An axisymmetric heat diffusion model was fitted to the measured TTR traces by adjusting the metal-to-diamond TBR, diamond film thermal conductivity and diamond-to-GaN TBR_{eff}; the diamond-to-GaN TBR_{eff} was found to be the most sensitive parameter for >100 ns after the heating laser pulse.

3. Thermal boundary resistance model

The model used in this work is adapted from the usual AMM explained in detail by Swartz *et al* [14]. Prasher and Phelan used a similar adaption of the AMM for weak interfaces but neglected phonon polarization mode conversion at the interface, assuming an effective phonon velocity for each mode [16]. Here, we use the full expression for weakly bonded interfaces presented by Schoenberg [15]; this has a different expression for each acoustic phonon polarization. There are two transverse and one longitudinal phonon polarization, described as SH, SV and P corresponding to transverse horizontal, transverse vertical and longitudinal (perpendicular)

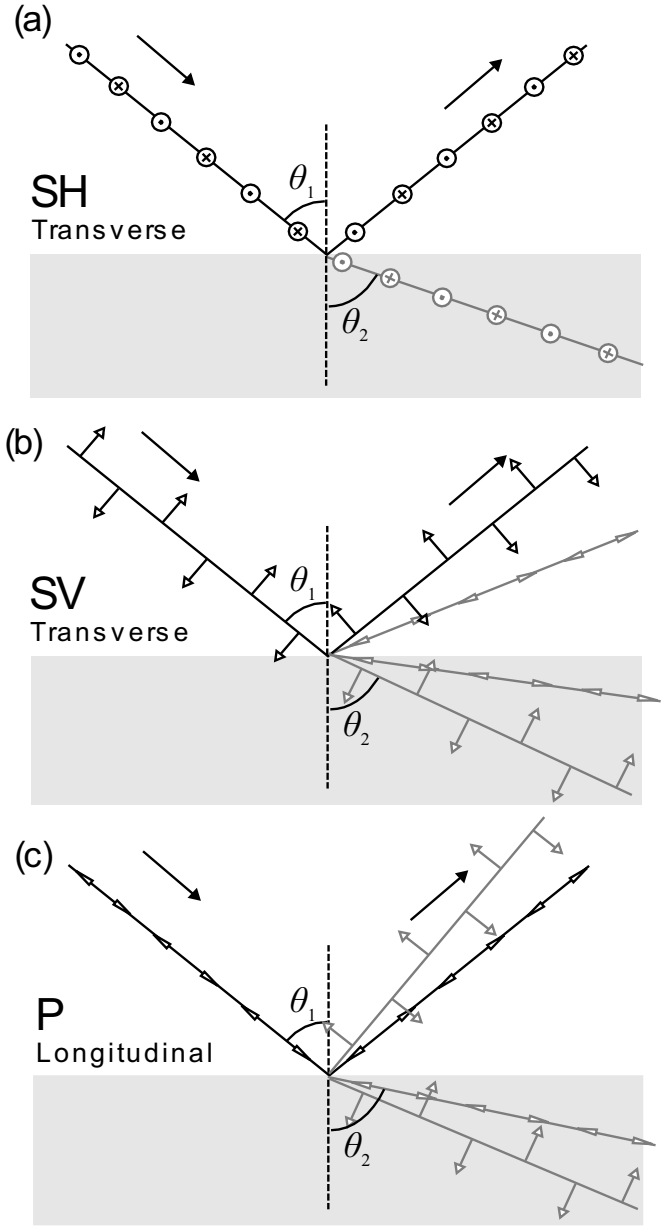

Figure 1. Sketches of phonon transmission and reflection at the interface between two solids. The second material (grey) has a higher phonon velocity. (a) A transverse phonon with polarization parallel to the interface, denoted SH for 'horizontal'; crosses and dots indicate displacement vector into and out of the page, respectively. (b) A transverse phonon polarized with a $\sin(\theta_1)$ component perpendicular to the interface, denoted SV for 'vertical'. (c) A longitudinal phonon with a $\cos(\theta_1)$ component perpendicular to the interface, denoted P. SV and P polarizations will undergo mode conversion depending on the angle of incidence, whereas SH phonons do not change into other modes.

modes, respectively. The transmission and reflection of these three modes is shown in figure 1. An SH phonon has a displacement vector polarized parallel to the interface, as shown in figure 1(a). An SH phonon is a special case that does not undergo mode conversion, with a transmission probability given by,

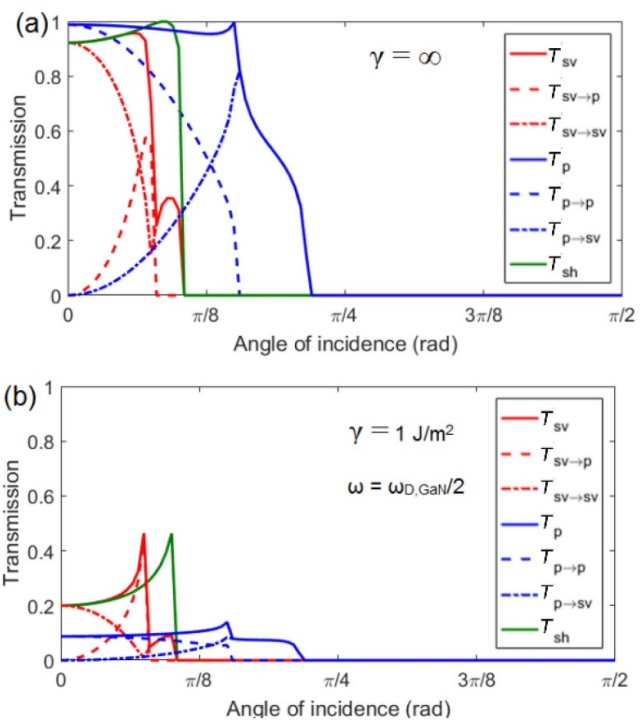

Figure 2. Transmission coefficients for phonons at the GaN/diamond interface. (a) For a welded interface and (b) for an interface with adhesion energy of 1 J m^{-2} and a phonon frequency of half the Debye frequency in GaN, $\frac{\omega_{D,GaN}}{2}$. Solid lines indicate the transmission probabilities for the three phonon polarizations. Dashed lines indicate those that transmit as P phonons. Dashed-dotted lines indicate the contribution that transmit as SV phonons. SH phonons do not convert into other phonon modes.

$$T_{SH\to SH} = \frac{4Z_{1,S}Z_{2,S}\cos\theta_1\cos\theta_2}{\left(Z_{1,S}\cos\theta_1 + Z_{2,S}\cos\theta_2\right)^2 + \frac{\omega^2}{K_A^2}\left(Z_{1,S}Z_{2,S}\cos\theta_1\cos\theta_2\right)^2} \quad (1)$$

where $Z_{i,S}$ is the acoustic impedance of material i for a transverse acoustic wave (S), ω is the phonon frequency and K_A is the spring constant per unit area of the interface. θ_1 is the angle of incidence and θ_2 is the angle of transmission. For all phonon polarizations, the angles of incidence, transmission and reflection are related by:

$$\frac{\sin\theta_{1,P}}{v_{1,P}} = \frac{\sin\theta_{2,P}}{v_{2,P}} = \frac{\sin\theta_{1,S}}{v_{1,S}} = \frac{\sin\theta_{2,S}}{v_{2,S}} \quad (2)$$

where $v_{i,j}$ is the phonon velocity in material i of mode j. Total internal reflection can occur when the phonon travels from a material with a lower acoustic velocity into a material with a higher velocity, *e.g.* $v_{1,j} < v_{2,j}$. This happens when the transmission angle becomes complex leading to a decaying transmission, or evanescent wave.

In general, the expressions for $T_{SV\to SV}$, $T_{SV\to P}$, $T_{P\to SV}$ and $T_{P\to P}$, are complex and are found by solving two sets of four linear equations of the displacement amplitudes. The derivation of these sets of equations is shown in [15]. Once these have been solved, the transmitted displacement amplitude from mode j to mode k, $t_{j\to k}$, can be converted into a

Table 1. Parameters used to calculate phonon transmission at the GaN/diamond interface, with material properties taken from the NSM archive [24].

Parameter	Value	Description
$v_{1,\mathrm{S}}$	8.04×10^3 (m s^{-1})	GaN transverse phonon velocity
$v_{1,\mathrm{P}}$	4.13×10^3 (m s^{-1})	GaN longitudinal phonon velocity
$v_{2,\mathrm{S}}$	17.52×10^3 (m s^{-1})	Diamond transverse phonon velocity
$v_{2,\mathrm{P}}$	12.82×10^3 (m s^{-1})	Diamond longitudinal phonon velocity
ρ_1	6150 (kg m^{-3})	GaN density
ρ_2	3515 (kg m^{-3})	Diamond density
$Z_{1,\mathrm{S}} = \rho_1 \cdot v_{1,\mathrm{S}}$	4.91×10^7 (Pa s m^{-3})	GaN transverse acoustic impedance
$Z_{1,P} = \rho_1 \cdot v_{1,P}$	2.54×10^7 (Pa s m^{-3})	GaN longitudinal acoustic impedance
$Z_{2,\mathrm{S}} = \rho_2 \cdot v_{2,\mathrm{S}}$	6.16×10^7 (Pa s m^{-3})	Diamond transverse acoustic impedance
$Z_{2,\mathrm{S}} = \rho_2 \cdot v_{2,\mathrm{S}}$	4.51×10^7 (Pa s m^{-3})	Diamond longitudinal acoustic impedance
ρ_{N_1}	4.4×10^{29} (m^{-3})	GaN atomic number density
ρ_{N_2}	1.77×10^{28} (m^{-3})	Diamond atomic number density
c_{GaN}	5.186×10^{-10} (m)	GaN lattice constant $\left(r_{0\_GaN} = \frac{3}{8} \cdot c_{GaN}\right)$
$a_{diamond}$	3.567×10^{-10} (m)	Diamond lattice constant $\left(r_{0\_di} = \sqrt{\frac{3}{4}} \cdot c_{diamond}\right)$

power transmission (or a probability of transmission) using the expression

$$T_{j\to k} = t_{j\to k}^2 \frac{Z_{2,k}\cos\theta_{2,k}}{Z_{2,k}\cos\theta_{1,j}}. \tag{3}$$

These probabilities have been plotted in figure 2 for two GaN-to-diamond interface cases: a 'welded' interface and a weakly bonded interface. There are four different angles of total internal reflection (TIR) corresponding to S → S, S → P, P → P and P → S. $T_{\mathrm{SH}\to\mathrm{SH}}$ has the same angle of TIR as $T_{\mathrm{SV}\to\mathrm{SV}}$ because the velocity of these transverse waves are assumed to be the same. From figure 2, at a transmission angle of zero the two transverse transmission probabilities are equal and there is no mode conversion for any incident phonon.

With a detailed model of the phonon transmission probability at a weakly bonded interface, we can calculate the TBR. Following Swartz and Pohl [14], the rate of energy crossing an interface per unit area, $\dot{Q}$, at temperature, T, is given by

$$\dot{Q}(T) = \frac{1}{2}\sum_{\mathrm{j}} \int_0^{\pi/2}\int_0^{\omega_D} \hbar\omega \cdot N_{1,j}(\omega, T) \cdot v_{1,j}\cos\theta_1 \cdot T_j \cdot \sin\theta_1 \mathrm{d}\theta_1 \mathrm{d}\omega \tag{4}$$

which averages over the phonon modes of each material, where the integral cutoff frequency ω_D is the Debye frequency of GaN, given by $k_B T_{D\_GaN}/\hbar$, where T_D is the Debye temperature of GaN (600 K). $N_{1,j}$ is the usual Debye phonon occupation in material 1 for mode j. Calculations are made at 300 K. The TBR is then calculated numerically using Fourier's law:

$$\mathrm{TBR} = \left(\frac{\mathrm{d}\dot{Q}}{\mathrm{d}T}\right)^{-1}. \tag{5}$$

To compare this model with experiment it is necessary to link the value of the spring constant per unit area, K_A, to the adhesion energy, γ. This can be done by assuming a Lennard-Jones (L-J) type potential for bonding at the interface. A L-J potential is a parameterized simplification of the vdW interaction potential between two atoms separated by r given by

$$\phi(r) = -4\varepsilon\left[\left(\frac{\sigma}{r}\right)^6 - \left(\frac{\sigma}{r}\right)^{12}\right] \tag{6}$$

where σ is a length scale and ε is the depth of the potential well. By considering the curvature at the equilibrium separation the effective spring constant, K, can be derived.

$$K = \left(\frac{\partial^2\phi}{\partial r^2}\right)_{r=r_0} = \frac{72\varepsilon}{2^{1/3}\sigma^2}. \tag{7}$$

This expression for K is valid for small displacements about the equilibrium position. Following the derivation by Yu *et al* [22], σ can be expressed in terms of the equilibrium nearest-neighbor atomic separation $\left(\sigma = 2^{-\frac{1}{6}} r_0\right)$ while γ can be expressed in terms of the number density of the atoms of the two bodies (ρ_{N_1}, ρ_{N_2}) and the Lennard-Jones parameters:

$$\gamma = \frac{\left(\frac{15}{2}\right)^{\frac{1}{3}}\varepsilon\pi^2\rho_{N\_1}\rho_{N\_2}\sigma^4}{4}. \tag{8}$$

By combining equations (7) and (8), and considering the total spring constant per unit area as $K_A = nK$, where n is the number of bonds per unit area at the interface, the spring constant per unit area of the interface is given by

$$K_A = n\left(\frac{576}{15^{1/3}\pi^2\rho_{N\_1}\rho_{N\_2}r_0^6}\right)\gamma. \tag{9}$$

The spring constant of the interface is proportional to the adhesion energy; the constant of proportionality can be calculated using known material properties. The atomic separation and the number of bonds per unit area is taken as an average of the two materials using the Lorentz–Berthelot mixing rule [23]. The parameters used in equations (1)–(9) are summarized in table 1, with specific values given for the GaN-to-diamond interface calculation.

4. Results and discussion

Figure 3 shows the transmission probability for different phonon frequencies at normal incidence to a GaN/diamond interface, together with the normalized phonon occupancy of GaN. Evidently, a weakly bonded interface acts as a low-pass filter for propagating phonons, allowing only the lowest energy phonons to pass. This greatly reduces the thermal conductance for weakly bonded interfaces. Typically, vdW bonding has an adhesion energy of <300 mJ m^{-2}, whereas a covalently bonded interface has an adhesion energy of 1000–2000 mJ m^{-2}, allowing a higher phonon transmission. Although not directly comparable to the thermodynamic energy of adhesion, the measured mechanical interface fracture toughness of GaN-on-diamond with a SiN interlayer is in the range 600–1000 mJ m^{-2} [9]. This is a range where the conventional DMM model is more applicable, *i.e.* the intrinsic TBR is predicted have a negligible contribution to the total thermal resistance.

Figure 4 shows the predicted dependence of the TBR on adhesion energy of a bonded GaN/diamond interface, calculated using the weakly bonded AMM (WB-AMM) model. At a typical van der Waals bond energy of around 300 mJ m^{-2}, *e.g.* the basal plane cleavage energy for graphite [25], the predicted TBR is 200 m^2 K GW^{-1}, which is 7× higher than the TBR_{eff} value measured for a 30 nm thick SiN interlayer in a GaN-on-diamond wafer [6]. This indicates that the direct growth of diamond on GaN (van der Waals bonding) is not a viable strategy for efficient thermal dissipation.

In comparison, figure 4 also shows that the intrinsic TBR of a covalently bonded layer is negligible. The measured $TBR_{di\text{-}GaN}$ value measured for the diamond-to-GaN film interface is 220 ± 70 m^2 K GW^{-1}, corresponding to the mean and standard deviation obtained from 7 measurements across the three wafers, closely matching the predicted WB-AMM TBR value. Formation of a strong covalent bond, *e.g.* a carbide bond for diamond, is therefore crucial for achieving low TBR GaN-on-diamond. Including a SiN (or other carbide forming) interlayer between the GaN and diamond is the best solution for minimizing thermal resistance. Reducing the thickness of the SiN and/or using alternative higher thermal conductivity crystalline materials, for example AlN [26], is the best strategy for minimizing TBR_{eff}.

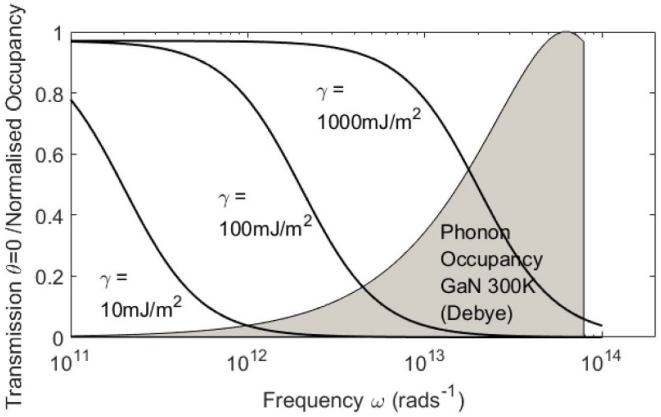

Figure 3. Transmission probability at the GaN/diamond interface as a function of frequency. The normalized phonon occupation in GaN at 300 K is also plotted for comparison. Weakly bonded interfaces act as a low-pass filter for phonons.

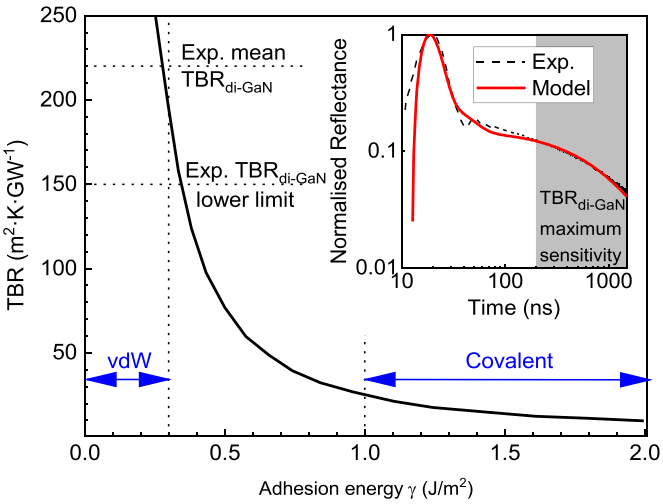

Figure 4. Predicted dependence of TBR with adhesion energy for a GaN/diamond interface using a weakly bonded-AMM model, with typical ranges indicated for van der Waals (vdW) and covalent adhesion energies. The measured average and lower limit TBR values are indicated on the vertical axis. Inset: a typical measured transient thermoreflectance trace and heat diffusion model fitted to obtain $TBR_{di\text{-}GaN}$.

5. Conclusions

We have implemented a weakly bonded TBR model to predict the intrinsic interfacial resistance of GaN-on-diamond, with TTR measurements used for experimental confirmation. Without an interlayer diamond only forms a weak van der Waals bond to GaN. This results in a TBR which is 7× higher than for GaN-on-diamond which includes a silicon nitride interlayer, negating the heat spreading benefit of diamond. A strong bond is crucial for the successful heterogeneous integration of GaN and diamond, despite the interlayer itself having a lower thermal conductivity and additional extrinsic thermal resistance. A suitable interlayer not only protects the GaN surface during growth [11], but also enables carbide bond formation which greatly increases the interface adhesion energy and consequently allows phonon transmission, acting as a 'phonon bridge' [27, 28].

Acknowledgments

This work was in part supported by the Engineering and Physical Sciences Research Council (EPSRC) Programme Grant GaN-DaME under EP/P00945X/1. We thank D. Liu (University of Bristol) for fruitful discussions.

ORCID iD

James W Pomeroy https://orcid.org/0000-0003-3443-8759

References

[1] Kim H G, Kihm K D, Lee W, Lim G, Cheon S, Lee W, Pyun K R, Ko S H and Shin S 2017 *Carbon* **125** 39–48
[2] Guerra V, Wan C and McNally T 2019 *Prog. Mater. Sci.* **100** 170–86
[3] Francis D, Faili F, Babic D, Ejeckam F, Nurmikko A and Maris H 2010 *Diam. Relat. Mater.* **19** 229–33
[4] Higurashi E, Okumura K, Nakasuji K and Suga T 2015 *Jpn. J. Appl. Phys.* **54** 030207
[5] Pomeroy J W, Bernardoni M, Dumka D C, Fanning D M and Kuball M 2014 *Appl. Phys. Lett.* **104** 083513
[6] Sun H R, Simon R B, Pomeroy J W, Francis D, Faili F, Twitchen D J and Kuball M 2015 *Appl. Phys. Lett.* **106** 111906
[7] Cheng Z, Yates L, Shi J, Tadjer M J, Hobart K D and Graham S 2019 *APL Mater.* **7** 031118
[8] Altman D *et al* 2014 *2014 IEEE Intsoc. Conf. Thermal (ITHERM)* pp 1199–205
[9] Liu D, Fabes S, Li B, Francis D, Ritchie R O and Kuball M 2019 *ACS Appl. Mater. Interfaces* **1** 354–69
[10] May P W 2000 *Phil. Trans. R. Soc.* A **358** 473–95
[11] May P W, Tsai H Y, Wang W N and Smith J A 2006 *Diam. Relat. Mater.* **15** 526–30
[12] Giri A, Braun J L and Hopkins P E 2016 *J. Phys. Chem.* C **120** 24847–56
[13] Lindroth D O and Erhart P 2016 *Phys. Rev.* B **94** 115205
[14] Swartz E T and Pohl R O 1989 *Rev. Mod. Phys.* **61** 605–68
[15] Schoenberg M 1980 *J. Acoust. Soc. Am.* **68** 1516–21
[16] Prasher R S and Phelan P E 2001 *Trans. ASME, J. Heat Transfer* **123** 105–12
[17] Prasher R 2018 *Nanosc. Microsp. Therm.* **22** 1–5
[18] Gotsmann B and Lantz M A 2013 *Nat. Mater.* **12** 59–65
[19] Das S, Lahiri D, Lee D-Y, Agarwal A and Choi W 2013 *Carbon* **59** 121–9
[20] Croot A, Wan G, Rowan A, Andrade H D, Smith J A and Fox N A 2017 *Front. Mech. Eng.* **3** 17
[21] Pomeroy J W, Simon R B, Sun H, Francis D, Faili F, Twitchen D J and Kuball M 2014 *IEEE Electron Device Lett.* **35** 1007–9
[22] Yu N and Polycarpou A A 2004 *J. Colloid. Interface Sci.* **278** 428–35
[23] Allen M P and Tildesley D J 2017 *Computer Simulation of Liquids* 2nd edn (Oxford: Oxford University Press)
[24] New Semiconductor Materials Archive (http://www.ioffe.ru/SVA/NSM/Semicond/)
[25] Wang W, Dai S, Li X, Yang J, Srolovitz D J and Zheng Q 2015 *Nat. Commun.* **6** 7853
[26] Kuball M, Pomeroy J W and Williams O A 2019 UK Patent No. GB 1814192.9
[27] English T S, Duda J C, Smoyer J L, Jordan D A, Norris P M and Zhigilei L V 2012 *Phys. Rev.* B **85** 035438
[28] Hu M, Zhang X L, Poulikakos D and Grigoropoulos C P 2011 *Int. J. Heat Mass Transfer* **54** 5183–91